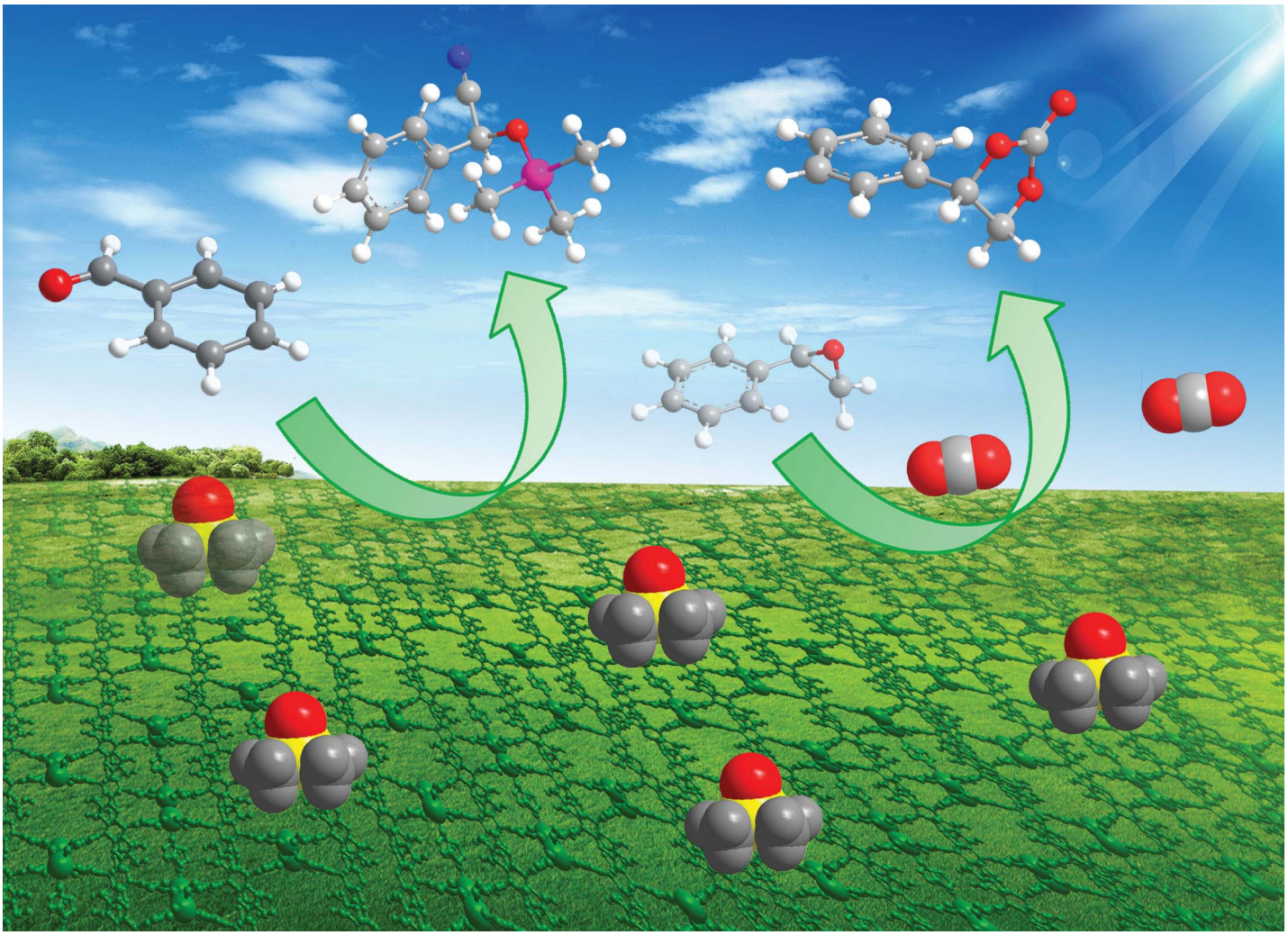

Showcasing the work of barium MOFs possessing efficient catalytic capacity and excellent fluorescence sensing ability presented by Prof. Daofeng Sun at State Key Laboratory of Heavy Oil Processing, China University of Petroleum (East China).

Title: Porous barium–organic frameworks with highly efficient catalytic capacity and fluorescence sensing ability

Highly active Ba^{2+} open metal sites can be generated through single-crystal-to-single-crystal transformation in porous barium-organic frameworks. These porous materials not only exhibit efficient catalytic capacity for the cyanosilylation of aldehydes/ketones, and the cycloaddition of CO_2 and epoxides, but also display high sensing ability for DMSO molecules through fluorescence enhancement.

As featured in:

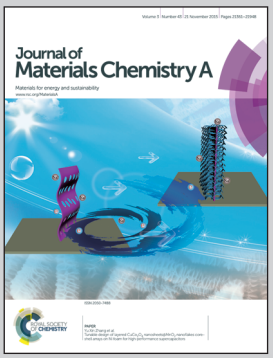

See Wenyue Guo, Daofeng Sun *et al.*, *J. Mater. Chem. A*, 2015, **3**, 21545.

ROYAL SOCIETY OF CHEMISTRY

www.rsc.org/MaterialsA

Registered charity number: 207890

Journal of Materials Chemistry A

PAPER

View Article Online
View Journal | View Issue

Cite this: J. Mater. Chem. A, 2015, 3, 21545

Porous barium–organic frameworks with highly efficient catalytic capacity and fluorescence sensing ability†

Fuling Liu,[b] Yuwen Xu,[a] Lianming Zhao,[a] Liangliang Zhang,[a] Wenyue Guo,*[a] Rongming Wang[a] and Daofeng Sun*[a]

Received 20th May 2015
Accepted 2nd August 2015

DOI: 10.1039/c5ta03680a

www.rsc.org/MaterialsA

The current study describes the first barium–organic framework with permanent porosity, efficient catalytic capacity, and highly selective luminescence sensing of DMSO molecules and metal ions. Single-crystal-to-single-crystal transformations (from complex **1** to complexes **2** and **3**) were used to thermally generate coordinatively unsaturated metal sites (CUSs) as catalytically active sites (CASs). Complex **3** exhibits efficient catalytic capacity for the cyanosilylation of aldehydes and ketones, and the cycloaddition of CO_2 and epoxides. To the best of our knowledge, complex **3** keeps a record among the MOF-based catalysts for the cyanosilylation of aldehydes and ketones. The generation of Ba^{2+} CUSs with high catalytic activity in a SCSC fashion is responsible for the excellent properties of **3**, which is further confirmed by the theoretical calculation. Besides, complex **2** can highly sense DMSO molecules through fluorescence enhancement.

Introduction

Porous MOFs with high thermal stability show potential applications in molecular separation, gas storage, catalysis and sensor devices.[1,2] In the past two decades, many porous MOFs with high surface area have been designed and synthesized, and their application in gas storage/separation has been widely and deeply studied.[3,4] The next challenges are to construct porous MOFs with capacities for heterogeneous catalysis and fluorescence sensors.[5,6] As is known, MOFs possess tunable channels/pores and specific functional groups acting as catalytically active sites (CASs) can be readily introduced.[7] For example, through introducing chiral small molecules as cooperative organocatalytic active sites into a Zn MOF, Duan *et al.* developed a new type of catalyst that can prompt the asymmetric α-alkylation of aliphatic aldehydes in a heterogeneous manner.[8] Another strategy for generating CASs in a MOF is to thermally release coordinated solvates on the metal center to generate coordinatively unsaturated metal sites (CUSs). In general, the CUSs in a MOF can act as a Lewis acid catalyst to catalyze cyanosilylation of aldehydes and ketones, and some other organic reactions such as the cycloaddition of CO_2 and epoxides. On the basis of the analysis of the reported results, the "naked" metal sites in a MOF can efficiently catalyze cyanosilylation of aldehydes and normally give a moderate or high yield.[9] However, low yields are observed for some cyanosilylations of aldehydes with substituent groups on the central benzene ring. Furthermore, the yields are much lower for the cyanosilylations of ketones.[10] For instance, a porous MOF based on 1,3,5-benzenetristetrazol-5-yl with exposed Mn^{2+} coordination sites as CASs can efficiently catalyze the cyanosilylations of benzaldehyde and 1-naphthaldehyde to give 98 and 90% yields, respectively. In contrast, for the cyanosilylations of acetophenone and 1-(naphthalen-1-yl)ethanone, the yields are only 28 and 1%, respectively, although the reaction time extends to 24 hours from 9 hours.[11] Besides the effect of steric hindrance, the reason may derive from the low activity or stability of CUSs. Hence, high activity and stability of CUSs are needed for the construction of functional MOFs with highly efficient catalytic capacity.

Recently, many porous MOFs with catalytic ability by the use of CUSs as catalytically active sites were documented. Most of the CUSs in the porous MOFs were limited to the first row transition metals such as Cu^{2+}, Mn^{2+}, Fe^{3+}, Co^{2+}, Ni^{2+}, Cr^{3+}, *etc.*[12,13] Surprisingly, porous materials based on s-block metals (alkali metals and alkaline earth metals) are relatively less explored,[14] which may be due to the lack of predictive coordination behavior of s-block metal centers.[15] Furthermore, it is normally difficult to form stable or fixed SBUs when s-block metal ions coordinate to

[a]State Key Laboratory of Heavy Oil Processing, China University of Petroleum (East China), College of Science, China University of Petroleum (East China), Qingdao, Shandong, 266580, People's Republic of China. E-mail: dfsun@upc.edu.cn; wyguo@upc.edu.cn

[b]Key Lab of Colloid and Interface Chemistry, Ministry of Education, School of Chemistry and Chemical Engineering, Shandong University, Jinan, Shandong, 250100, People's Republic of China

† Electronic supplementary information (ESI) available: Experimental details, TGA, PXRD and the solid-state luminescence emission spectra of **1** and **2**, and additional figures. CCDC 981821–981823. For ESI and crystallographic data in CIF or other electronic format see DOI: 10.1039/c5ta03680a

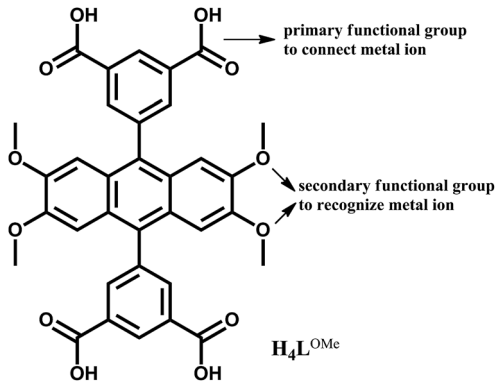

Scheme 1 The tetracarboxylate ligand in this work.

carboxylate ligands. However, these porous MOFs based on s-block metal ions with CUSs may generate functional materials with highly efficient catalytic capacity.

Another potential application of CUSs in porous MOFs is the fluorescence sensing of small molecules. Recently, much effort has been made for rational design and synthesis of porous MOFs for sensing ions and organic molecules. Several recent reviews have highlighted the exciting and compelling developments in porous MOF-based chemical sensors.[16] In particular, sensing metal ions or organic small molecules using porous MOFs with open metal sites or Lewis basic sites has been documented by Chen, Li and other groups.[17] However, highly selective luminescence sensing of organic molecules or metal ions by porous MOFs based on s-block metals has been seldom reported so far. In this paper, we describe, for the first time, the synthesis and single-crystal-to-single-crystal transformation of barium–organic frameworks with permanent porosity, efficient catalytic capacities, and highly selective sensing of organic molecules and metal ions.

The solvothermal reaction of 5,5′-(2,3,6,7-tetramethoxyanthracene-9,10-diyl)diisophthalic acid ($\mathbf{H_4L^{OMe}}$, Scheme 1) and $Ba(NO_3)_2$ salt resulted in the formation of a microporous barium–organic framework, $Ba_2(\mathbf{H_2L^{OMe}})_2(NMP)\cdot NMP$ (**1**), with high thermal stability. When heated at 325 °C, **1** can transform to **2**, $[Ba(\mathbf{H_2L^{OMe}})_{0.5}(H_2O)\cdot 4H_2O]_n$, through a single-crystal-to-single-crystal transformation. It is interesting to find that the porous material of **2** can highly sense DMSO molecules through fluorescence enhancement. Fortunately, the intermediate (**3**) from the transformation of **1** to **2** was captured and characterized by single-crystal X-ray diffraction. Complex **3** exhibits high catalytic ability for the cyanosilylation of aldehydes and ketones, as well as the cycloaddition of CO_2 and epoxides. The existence of highly active Ba^{2+} open metal sites in the framework is responsible for the highly efficient catalytic capacity of **3**, which is further confirmed by the theoretical calculation.

Experimental

Materials and methods

All chemicals and solvents used in the syntheses were of analytical grade and used without further purification. The ligand $\mathbf{H_4L^{OMe}}$ was prepared according to the ESI.† Elemental analyses (C, H, N) were performed on a PerkinElmer 240 elemental analyzer. The thermogravimetric analysis (TGA) of complexes **1** and **2** was carried out between room temperature and 600 °C in static N_2 with a heating rate of 10 °C min^{-1}. Photoluminescence spectra were measured on an F-280 fluorescence spectrophotometer. Low pressure (<800 torr) gas (N_2, CO_2 and CH_4) sorption isotherms were measured using a Micrometrics ASAP 2020 surface area and pore size analyzer. ^{1}H NMR spectra were measured on a Bruker AVANCE-300 NMR Spectrometer.

Synthesis of MOFs

Synthesis of 1. A mixture of $Ba(NO_3)_2$ (20 mg, 0.07 mmol) and $\mathbf{H_4L^{OMe}}$ (3 mg, 0.005 mmol) was dissolved in NMP/DMA/H_2O mixed solvents (1 mL, v/v/v 1/1/1). Then, the solution was sealed in a pressure-resistant glass tube, slowly heated to 130 °C from room temperature in 8 hours, kept at 130 °C for 50 hours, and then slowly cooled to 30 °C in 13 hours. The dark red crystals that formed were collected and dried in air (yield: 57%, based on barium.). Their purity was confirmed by X-ray powder diffraction (XRD). Elemental analysis (%) of **1**: calcd: C 54.40, H 3.86, and N 1.63; found: C 52.62, H 3.85, and N 1.50.

Synthesis of 2. The as-synthesized crystals of **1** were heated at 325 °C for 20 minutes in air, and then cooled to room temperature to generate **2**. Elemental analysis (%) of **2**: calcd: C 47.93 and H 4.02; found: C 46.77 and H 3.51.

Capture of intermediate 3. The crystals of **2** were heated at 127 °C for 1 hour to generate intermediate **3**, whose crystal data were collected at 127 °C. **3** can only exist at high temperature, and **3** can transform to **2** immediately in air when the temperature decreases to room temperature.

X-ray structure determination and structure refinement

Single-crystal X-ray diffraction of **1** and **2** was performed using a Bruker Apex II CCD diffractometer equipped with a fine-focus sealed-tube X-ray source (Mo Kα radiation), and the crystal data of **3** were collected on an Agilent Xcalibur Eos Gemini diffractometer with an enhanced (Cu) X-ray source (Cu-Kα, $\lambda = 1.54178$ Å). Structures were solved by direct methods using SHELXTL and were refined by full-matrix least-squares on F^2 using SHELX-97. Contributions to scattering from all solvent molecules were removed using the SQUEEZE routine of PLATON; structures were then refined again using the data generated. Crystal data of **1**: triclinic, $P\bar{1}$, $a = 9.0362(15)$ Å, $b = 17.484(3)$ Å, $c = 24.772(4)$ Å, $\alpha = 69.717(3)°$, $\beta = 84.873(3)°$, $\gamma = 82.904(3)°$, and $V = 3638.3(10)$ Å^3; $Z = 2$; calculated cell density, $D_c = 1.481$ g cm^{-3}; reflections collected/independent: 18 155/12 676; $R_{int} = 0.0834$; final $R_1 = 0.1012$, w$R_2 = 0.2099$, and GOF = 1.051. Crystal data of **2**: monoclinic, $C2/c$, $a = 32.24(5)$ Å, $b = 12.209(19)$ Å, $c = 8.885(13)$ Å, $\beta = 97.56(3)°$, and $V = 3467(9)$ Å^3; $Z = 4$; calculated cell density, $D_c = 1.494$ g cm^{-3}; reflections collected/independent: 7731/2978; $R_{int} = 0.0849$; final $R_1 = 0.1383$, w$R_2 = 0.2241$, and GOF = 1.013. Crystal data of **3**: monoclinic, $C2/c$, $a = 32.2746(7)$ Å, $b = 12.6358(6)$ Å, $c = 8.9507(2)$ Å, $\beta = 98.533(2)°$, and $V = 3609.8(2)$ Å^3; $Z = 4$;

calculated cell density, $D_c = 1.402$ g cm^{-3}; reflections collected/independent: 12 228/3429; $R_{int} = 0.0604$; final $R_1 = 0.0718$, w$R_2 = 0.1625$, and GOF = 1.046.†

Results and discussion

Single-crystal-to-single-crystal transformation

The single-crystal X-ray diffraction study reveals that **1** is a three-dimensional porous framework based on a 1D barium rod-shaped SBU. The organic ligand of $\mathbf{H_4L^{OMe}}$ was partly deprotonated during the solvothermal reaction. There are two types of barium ions with different coordination environments. Ba1 is coordinated by eight oxygen atoms from $\mathbf{H_4L^{OMe}}$ ligands and one NMP molecule, and Ba2 is coordinated by eight oxygen atoms from $\mathbf{H_4L^{OMe}}$ ligands. Thus, the barium ions are connected by carboxylate groups generating infinite Ba–O–C rods along the [1 0 0] direction with the nearest Ba–Ba distance of 4.937 Å. In the rod-shaped SBU, the protonated carboxylate groups formed strong hydrogen bonds with the adjacent deprotonated carboxylate groups to further stabilize the SBU (Fig. 1). The Ba–O–C rods are stacked in parallel and linked by the backbone of $\mathbf{H_4L^{OMe}}$ forming two kinds of 1D channels along the *a* axis with the dimensions of 8.5 × 9.0 Å for channel A, in which uncoordinated solvates reside, and 8.0 × 11.5 Å for channel B, in which coordinated NMP molecules reside (Fig. 1). The solvent-accessible volume of **1** is 21.5% calculated with PLATON after the removal of the coordinated NMP molecules.[18] To check the permanent porosity of **1**, the freshly prepared samples were soaked in methanol to exchange the less volatile solvent, followed by evacuation under dynamic vacuum at 90 °C overnight. Desolvated **1** displays typical type-I adsorption isotherms with a Brunauer–Emmett–Teller (BET) surface area of 310.6 m^2 g^{-1}, suggesting the retention of the microporous structure after the removal of solvents from the crystalline samples (Fig. S7–S9†). Actually, the crystal structure of the desolvated **1** was also determined through single-crystal X-ray diffraction (see below).

Thermogravimetric analysis indicates that the coordinated NMP molecules are completely released before 325 °C and **1** can be stable up to 400 °C. When heated at 325 °C for 20 minutes and then cooled to room temperature, **1** can transform to **2** through single-crystal-to-single-crystal transformation. Normally, porous MOFs possess lower thermal stability and when heated at high temperature, most of them will lose their crystallinity. The SCSC transformation at high temperature like complex **1** is quite rare. The crystal system changes from triclinic for **1** to monoclinic for **2**, indicating that the symmetry increases. The central barium ion in **2** is nine-coordinated by eight oxygen atoms from five $\mathbf{H_4L^{OMe}}$ ligands and one aqua ligand, suggesting the coordinated NMP molecule on barium in **1** was replaced by a water molecule. Furthermore, the eight-coordinated barium ion in **1** changed to the nine-coordinated barium ion in **2**. Thus, the 3D porous framework of complex **2** possesses only one kind of channel, in which coordinated water molecules reside (Fig. 1d). The solvent-accessible volume of **2** is 18.3% calculated with PLATON after the removal of the coordinated water molecules.

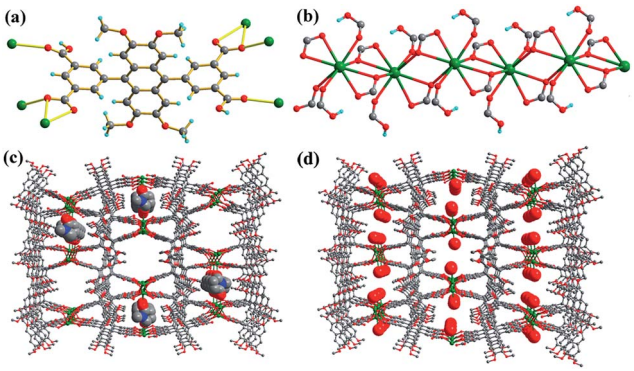

Fig. 1 (a) The coordination mode of the ligand in **1**. (b) The 1D rod-shaped SBU in **1**. (c) The 3D open framework of **1** with the coordinated NMP in a space-filling mode. (d) The 3D porous framework of **2** showing coordinated water molecules in the channels.

Fortunately, the intermediate of the transformation from **1** to **2** was captured. The coordinated water molecules on the barium ion in **2** can be removed to generate the intermediate **3** when heated at 400 K. The crystal data of **3** were collected at 400 K and the careful refinement of the crystal data can give good crystallographic parameters including the *R* value. Complex **3** possesses a similar structure to **2**, except that the central barium ions in **3** are eight-coordinated. The solvent-accessible volume of **3** is 19.1% calculated with PLATON. Complex **3** only exists at high temperature. When cooled to room temperature, **3** can transform to **2** again. Thus, complex **3** should be the intermediate between **1** and **2**. More interestingly, the coordinated water molecules can lead to the color change significantly. As shown in Fig. 2, the crystal color of **2** is deep brown; however, after the removal of the coordinated water molecules to generate **3**, the color changed to yellow (Fig. 2), and the transformation is reversible. In the past decades, although many single-crystal-to-single-crystal transformations based on MOFs have been reported, the SCSC transformation including a color change induced by the change in the metal coordination geometry is still rare.[19]

Catalytic properties

Considering the high thermal stability and the existence of CUSs in **3**, the Lewis acid-catalyzed reactions of carbonyl compounds with cyanide, and the cycloaddition of CO_2 and epoxides were carried out. The freshly prepared sample of **3** was used for the catalytic test.

Cyanosilylation of aldehydes and ketones. Cyanohydrins, which can be synthesized by cyanosilylation of aldehydes and ketones, are a class of important organic intermediates for both biological processes and synthetic chemistry.[20] On the basis of the current research, most of the porous MOFs with open metal sites can catalyze the cyanosilylation of benzaldehyde and give a high yield, but for benzaldehyde with substituent groups, low yield can normally be observed. However, in this work, compound **3** displays high activity not only for benzaldehyde but also for the derivative of benzaldehyde. As shown in Table 1,

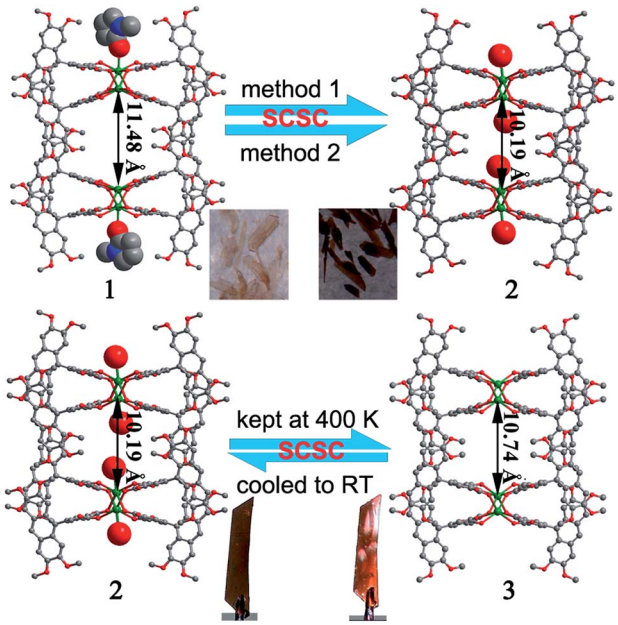

Fig. 2 The SCSC transformations among **1**, **2** and **3**. Method 1: crystals of **1** were immersed into methanol for 2 days, then heated at 360 K and cooled to R.T. Method 2: crystals of **1** were heated directly to 598 K for 20 minutes, and then cooled to R.T.; SCSC represents single-crystal-to-single-crystal transformation.

complex **3** shows high activity in the cyanosilylation of benzaldehyde, and the conversion can reach completion within 2 h. For some aldehydes with electron-donating or electron-withdrawing groups (Table 1, entries 2–7), almost 100% yields were also reached after 2 h at room temperature, which outperform some MOF catalysts. For example, Nd(btc)-MOFs afforded 88% conversion of benzaldehyde but only 18% of α-naphthaldehyde.[21a] As is well known, for the cyanosilylation of ketones,[21] the yields were normally lower than those of the cyanosilylation of aldehydes due to the steric hindrance and the lower activity of ketones. For instance, Sc-MOF, Cu-DDQ and CPO-27-Mn catalyzed benzaldehyde with high conversions of 90%, 95% and 100%, respectively; however, the conversions of acetophenone are 55%, 7% and 17%, respectively.[21b–d] Unlike them, complex **3** also shows excellent activity in the cyanosilylation of ketones. The yields of some ketones such as acetophenone, *p*-methylacetophenone, *para*-chloroacetophenone, *p*-nitroacetophenone, and 4-phenylbut-3-en-2-one can be obtained at almost 100% within 2 h at room temperature (Table 1, entries 8–12). For propiophenone and larger 1-(naphthalen-1-yl)ethanone, the yields can still reach ~100% in 2 h, further indicating the high catalytic activity of **3**. Moreover, the turnover number (TON) and the turnover frequency (TOF) for the cyanosilylation of benzaldehyde can reach 192 and 384 h^{-1}, respectively, which are much higher than other reported results (Table S3†).[21] These excellent catalytic results make complex **3** a record in the cyanosilylation of aldehydes and ketones among the reported MOF-based catalysts. The catalytic capacity of **3** is even much higher than that of polymer-supported metal complexes and $SbCl_3$-based catalysts.[22] Besides, to demonstrate its recyclability, successive reactions of **3** were carried out for the cyanosilylation of benzaldehyde, showing that the yield of benzaldehyde remains at ~100% without any loss of catalytic activity for three cycles at least (Fig. S10†).

Cycloaddition of CO_2 and epoxides. To further explore the catalytic performance of **3** as a Lewis acid, we decided to use the reaction of the cycloaddition of CO_2 and epoxides to form cyclic carbonates, since CO_2 is considered as a cheap C-1 source for the preparation of various chemicals and cyclic organic carbonates.[23] Recently, porous MOF materials with open metal sites have been proved to be efficient heterogeneous catalysts for the cycloaddition of CO_2 and epoxides because these materials can catalyze the cycloaddition under relative mild conditions.[24] For instance, MIL-68(In) and MIL-68(In)–NH_2 demonstrate catalytic activity for the cycloaddition of 2-phenyloxirane with CO_2 at 150 °C under 0.8 MPa CO_2 pressure within 8 h with yields of 36% and 48%, respectively.[24a] Ni(salphen)-MOFs catalyzed 2-(phenoxymethyl)oxirane with CO_2 at 80 °C under 2 MPa CO_2 pressure over 8 h with a yield of 55%.[24b] However, as shown in Table 2, complex **3** demonstrates highly efficient catalytic activity for the reaction of CO_2 and epoxides such as 2-phenyloxirane, 2-(phenoxymethyl)oxirane, and 2-decyloxirane and the yields for each reaction are above 80% over 4 hours at 80 °C under 0.6 MPa CO_2 pressure, which are much higher than the results mentioned above.[24] Although several MOF-based catalysts exhibiting higher yields than that of **3** were reported,[25] these catalytic experiments were run under the conditions with much higher CO_2 pressure and temperature. Considering the high yields of cycloaddition of CO_2 and epoxides at low temperature and pressure, complex **3** possesses significant advantages for chemical fixation of CO_2 and preparation of cyclic organic carbonates.

Theoretical calculation. It is well known that cyanosilylation of aldehydes and ketones is a class of organic reactions catalyzed by a Lewis acid. In the case of **3**, the possible mechanism for the cyanosilylation reaction is shown in Scheme 2. Considering the highly efficient catalytic capacity of 3 in the cyanosilylation of aldehydes and ketones, density functional theoretical (DFT) calculations were performed based on a cluster model (Ba-**3**) *via* the adsorption of benzaldehyde (Fig. S11 and Table S6†) to evaluate the Lewis acid sites in **3**. When the benzaldehyde molecule is adsorbed through the O end, it is located at the Ba top site with the Ba–O distance of 2.910 Å. The corresponding adsorption energy is calculated to be 18.8 kcal mol^{-1}, and thus indicates a strong bonding between benzaldehyde and Ba-**3**. Upon adsorption on Ba-**3**, it is found that there is 0.08|*e*| transferred from the adsorbed benzaldehyde molecule to the Ba-**3** cluster, while the natural bond orbital (NBO) charge on Ba changes from 1.36 to 1.28|*e*| with the formation of the C_6H_5CHO–Ba-**3** complex. All these results suggest that the Ba atom in Ba-**3** serves as a strong Lewis acid site. Furthermore, due to a positive charge distribution on the Ba atom (1.36|*e*|), the adsorption of benzaldehyde on it *via* the O end could strengthen the polarization of the aldehyde C–O localized molecular orbitals, and thus lead to a weaker C–O covalent bonding in C_6H_5CHO–Ba-**3**, which is confirmed by the elongation of the aldehyde C–O bond from 1.222 Å in free

Table 1 Cyanosilylation of a variety of aldehydes and ketones catalyzed by 3

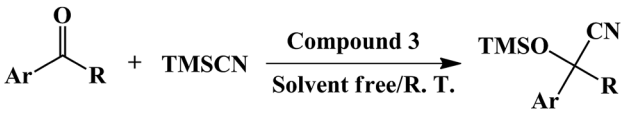

Entry	Aldehyde/ketone	Product	Time (h)	Yield[c] (%)
1[a]	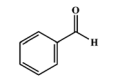	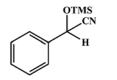	2	100
2[a]	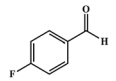	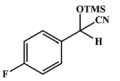	2	100
3[a]	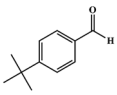	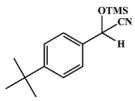	2	100
4[a]	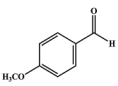	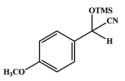	2	100
5[a]	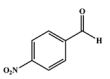	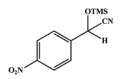	2	100
6[a]	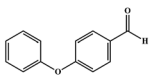	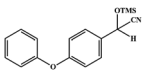	2	100
7[a]		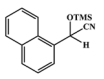	2	100
8[b]			2	100
9[b]		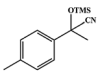	2	100
10[b]		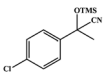	2	100
11[b]	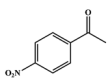	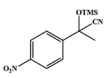	2	100
12[b]	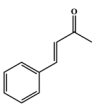	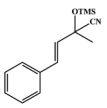	2	100
13[b]		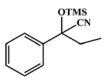	2	100
14[b]		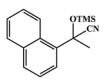	2	100

[a] Reaction conditions: TMSCN (4 mmol), aldehyde (2 mmol), 3 (7.8 mg, 0.01 mmol), room temperature, and under N_2. [b] Reaction conditions: TMSCN (2 mmol), ketone (0.5 mmol), 3 (7.8 mg, 0.01 mmol), room temperature, and under N_2. [c] Determined by ^{1}H NMR based on the carbonyl substrate.

Table 2 Yields for 3-catalyzed cycloaddition of CO_2 and epoxides[a]

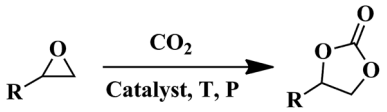

Entry	Epoxides	Product	Time (h)	Yield[b] (%)
1	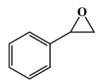	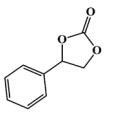	4	80
2	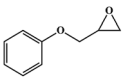	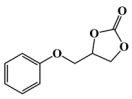	4	98
3	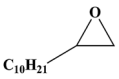	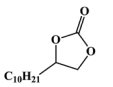	4	89

[a] Reaction conditions: substrate (15 mmol), TBAB (1 mmol), 3 (15 mg, 0.02 mmol), 80 °C under 0.6 MPa CO_2 pressure. [b] Calculated by GC.

benzaldehyde to 1.230 Å in C_6H_5CHO–Ba-3. Further NBO analysis shows that when benzaldehyde is adsorbed on Ba-3, the charges on aldehyde O and C increase to −0.56 and 0.43|e| from −0.53 and 0.39|e| in free benzaldehyde (Table 3), respectively. The apparent increase of positive charges on aldehyde C favors further cyanosilylation of benzaldehyde.

Fluorescence sensing properties. The solid-state luminescent emission spectra of **1**, **2** and $\mathbf{H_4L^{OMe}}$ were studied at room temperature (Fig. S5 and S6†). $\mathbf{H_4L^{OMe}}$ and **1** have slightly different emissions at 467 and 506 nm upon 270 and 360 nm excitations, respectively, which can be ascribed to the $\pi^* \rightarrow n$ or $\pi^* \rightarrow \pi$ electronic transitions. However, the emission spectra of **2** are at 345 nm upon 230 nm excitation, 122 and 161 nm blue shift compared to $\mathbf{H_4L^{OMe}}$ and **1**, respectively. In this case, the emission of **2** can probably be assigned to metal-to-ligand

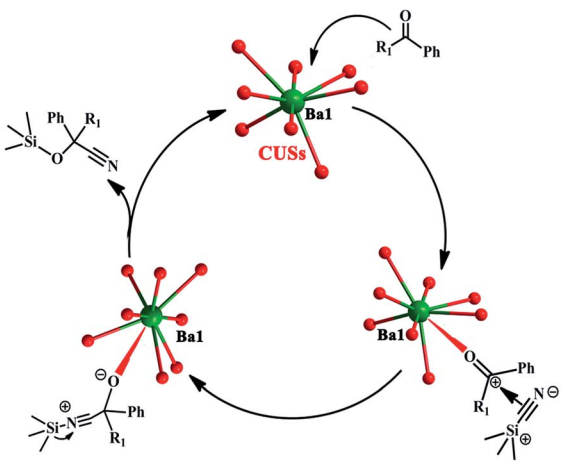

Scheme 2 The possible mechanism for the cyanosilylation of aldehydes and ketones in the case of 3.

Table 3 Calculated NBO charges on different atoms of C_6H_5CHO, Ba-3, and C_6H_5CHO–Ba-3 (unit of |e|)

Species	C_6H_5CHO	Ba-3	C_6H_5CHO–Ba-3
C_6H_5CHO	0		0.08
C1	0.39		0.43
O1	−0.53		−0.56
Ba1		1.36	1.28

charge transfer (MLCT) or ligand-to-metal charge transfer (LMCT).[26]

More interestingly, **1** and **2** show different responses to small organic molecules. Complex **2** can selectively sense DMSO molecules through fluorescence enhancement, whereas **1** cannot. To examine the potential of **2** for the sensing of small molecules, we select toluene as the standard emulsion. The as-synthesized sample of **2** was ground and suspended in toluene solution, and different organic molecules (DMSO, DMF, methanol, ethanol, 1-propanol, 2-propanol, hexane, acetone, dichloromethane, THF, and acetonitrile) were dropwise added. The luminescent properties are recorded and listed in Fig. 3. Interestingly, most of the organic molecules have slight effects on the luminescence intensity, except for DMSO. For example, with the dropwise addition of methanol, ethanol, 2-propanol, hexane, acetone, dichloromethane, THF, and acetonitrile, the luminescence intensities increase slightly. With the addition of DMF and 1-propanol, the luminescence intensities increase 6 and 4 times, respectively, compared to the original one. However, addition of DMSO molecules to the toluene emulsion of **2** led to a significant increase of its luminescence intensity, and the enhancement attained saturation when about 0.7 mL DMSO was added. The maximum of the luminescence intensity is about 41 times greater than the original one, indicating that **2** exhibits high selectivity for sensing DMSO molecules through fluorescence enhancement. In contrast, addition of DMSO molecules to the toluene emulsion of **1** led to a slight increase of its luminescence intensity, indicating there is no selectivity to DMSO molecules for **1**. Although detailed study of the mechanism is still needed, gradual replacement of coordinated water molecules on the barium sites by DMSO molecules is crucial to fluorescence enhancement.[17a]

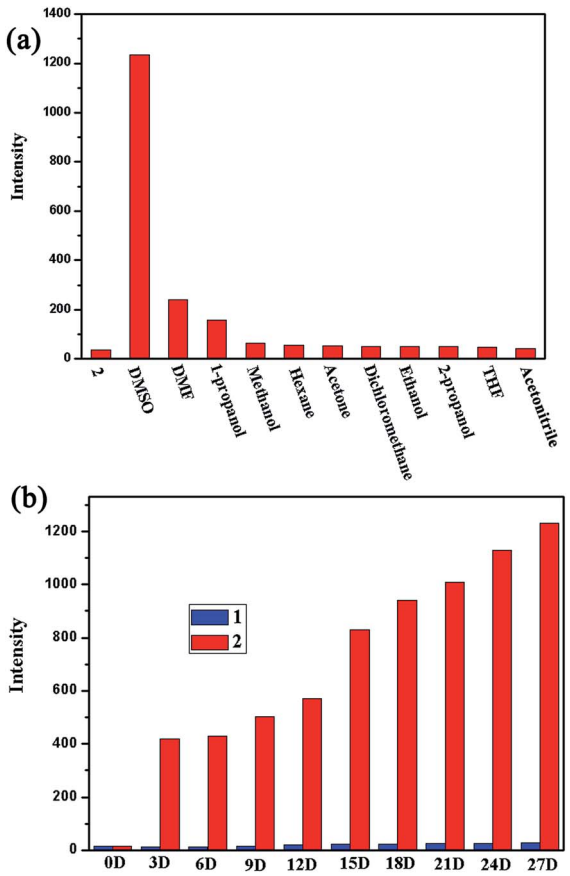

Fig. 3 (a) Photoluminescence intensities of **2** introduced into various organic solvents (excited at 380 nm), showing high selectivity for DMSO molecules. (b) Comparison of the selectivities to DMSO molecules for **1** and **2**.

Due to the existence of dimethoxy groups that point toward the channels and can chelate metal ions,[27] the sensing of metal ions by **2** emulsion was also carried out. The freshly prepared sample of **2** was ground and dispersed in a DMF solvent to generate a 2-DMF emulsion, into which different metal ions were added. Upon the addition of Mg^{2+}, Ca^{2+}, and K^{+} cations, the luminescence intensities increased slightly, and the opposite results were observed for the addition of Cd^{2+}, Mn^{2+}, and Zn^{2+} cations. However, the luminescence intensities decreased significantly upon the addition of Co^{2+}, Pb^{2+}, Cu^{2+}, and Ni^{2+} cations, suggesting the selective sensing of these metal ions through fluorescence quenching (Fig. S34 and S35†).

Conclusions

In conclusion, a microporous barium–organic framework (**1**) based on a new anthracene-functionality tetracarboxylic acid was synthesized and characterized. When heated at 598 K to thermally release coordinated NMP molecules and cooled to room temperature, **1** can transform to **2** through single-crystal-to-single-crystal (SCSC) transformation involving the change of the coordination number of the central metal ion. Fortunately, the intermediate (**3**) of this SCSC transformation was also obtained when **2** was heated to 400 K. Although complexes **1** and **2** possess similar structures, they exhibit different luminescent responses to DMSO molecules. **2** can highly sense DMSO molecules through fluorescence enhancement, whereas **1** cannot. More interestingly, complex **3** possesses highly efficient catalytic capacities in the cyanosilylation of aldehydes and ketones, and the cycloaddition of CO_2 and epoxides due to the existence of Ba^{2+} CUSs with high activity, which was confirmed by theoretical simulation. To the best of our knowledge, there is no report on porous Ba MOFs with high thermal stability, SCSC transformation, and exhibiting high catalytic activity. These results presented here indicate that Ba^{2+} CUSs may possess high activity for some organic reactions, which provide a new strategy for the design and synthesis of porous materials with highly efficient catalytic capacity.

Acknowledgements

This work was supported by the NSFC (Grant No. 21001115, 21271117), NCET-11-0309, the Shandong Natural Science Fund for Distinguished Young Scholars (JQ201003), and the Fundamental Research Funds for the Central Universities (13CX05010A).

Notes and references

1 (*a*) H. C. Zhou, J. R. Long and O. M. Yaghi, *Chem. Rev.*, 2012, **112**, 673–674; (*b*) K. Sumida, D. L. Rogow, J. A. Mason, T. M. McDonald, E. D. Bloch and Z. R. Herm, *Chem. Rev.*, 2012, **112**, 724–781; (*c*) L. E. Kreno, K. Leong, O. K. Farha, M. Allendorf, R. P. van Duyne and J. T. Hupp, *Chem. Rev.*, 2012, **112**, 1105–1125.

2 (*a*) R. Haldar, R. Matsuda, S. Kitagawa, S. J. George and T. K. Maji, *Angew. Chem., Int. Ed.*, 2014, **53**, 11772–11777; (*b*) M. Zhang, G. X. Feng, Z. G. Song, Y. P. Zhou, H. Y. Chao, D. Q. Yuan, T. T. Y. Tan, Z. G. Guo, Z. G. Hu, B. Z. Tang, B. Liu and D. Zhao, *J. Am. Chem. Soc.*, 2014, **136**, 7241–7244; (*c*) S. S. Nagarkar, B. Joarder, A. K. Chaudhari, S. Mukherjee and S. K. Ghosh, *Angew. Chem., Int. Ed.*, 2013, **52**, 2881–2885; (*d*) A. J. Lan, K. H. Li, H. H. Wu, D. H. Olson, T. J. Emge, W. Ki, M. C. Hong and J. Li, *Angew. Chem., Int. Ed.*, 2009, **48**, 2334–2338.

3 (*a*) Z. J. Zhang, W. Y. Guo, L. Wojtas, S. Q. Ma, M. Eddaoudi and M. J. Zaworotko, *Angew. Chem., Int. Ed.*, 2012, **51**, 9330–9334; (*b*) S. T. Zheng, J. T. Bu, Y. F. Li, T. Wu, F. Zuo, P. Y. Feng and X. H. Bu, *J. Am. Chem. Soc.*, 2010, **132**, 17062–17064; (*c*) H. Furukawa, N. Ko, G. Y. B. Aratani, N. Aratani, S. B. Choi, E. Choi, A. Ö. Yazaydin, R. Q. Snurr, M. O'Keeffe, J. Kim and O. M. Yaghi, *Science*, 2010, **329**, 424–428.

4 (*a*) Q. P. Liu, T. Wu, S. T. Zheng, X. H. Bu and P. Y. Feng, *J. Am. Chem. Soc.*, 2012, **134**, 784–787; (*b*) B. S. Zheng, J. F. Bai, J. G. Guan, L. Wojtas and M. J. Zaworotko, *J. Am. Chem. Soc.*, 2011, **133**, 748–751; (*c*) D. W. Lim, S. A. Chyun and M. P. Suh, *Angew. Chem., Int. Ed.*, 2014, **53**, 7819–7822.

5 (*a*) J. Y. Lee, O. K. Farha, J. Roberts, K. A. Scheidt, S. T. Nguyen and J. T. Hupp, *Chem. Soc. Rev.*, 2009, **38**, 1450–1459; (*b*) A. U. Czaja, N. Trukhan and U. Muller, *Chem. Soc. Rev.*, 2009, **38**, 1284–1293; (*c*) J. W. Liu, L. F. Chen, H. Cui, J. Y. Zhang, L. Zhang and C. Y. Su, *Chem. Soc. Rev.*, 2014, **43**, 6011–6061.

6 (*a*) K. Mo, Y. H. Yang and Y. Cui, *J. Am. Chem. Soc.*, 2014, **136**, 1746–1749; (*b*) J. M. Falkowski, T. Sawano, T. Zhang, G. Tsun, Y. Chen, J. V. Lockard and W. B. Lin, *J. Am. Chem. Soc.*, 2014, **136**, 5213–5216; (*c*) K. Manna, T. Zhang and W. B. Lin, *J. Am. Chem. Soc.*, 2014, **136**, 6566–6569; (*d*) X. Jing, C. He, D. P. Dong, L. L. Yang and C. Y. Duan, *Angew. Chem., Int. Ed.*, 2012, **51**, 10127–10131.

7 (*a*) D. B. Dang, P. Y. Wu, C. He, Z. Xie and C. Y. Duan, *J. Am. Chem. Soc.*, 2010, **132**, 14321–14323; (*b*) B. Y. Li, Y. M. Zhang, D. X. Ma, L. Li, G. H. Li, G. D. Li, Z. Shi and S. H. Feng, *Chem. Commun.*, 2012, **48**, 6151–6153.

8 P. Y. Wu, C. He, J. Wang, X. J. Peng, X. Z. Li, Y. L. An and C. Y. Duan, *J. Am. Chem. Soc.*, 2012, **134**, 14991–14999.

9 (*a*) K. Mo, Y. H. Yang and Y. Cui, *J. Am. Chem. Soc.*, 2014, **136**, 1746–1749; (*b*) S. Horike, M. Dincă, K. Tamaki and J. R. Long, *J. Am. Chem. Soc.*, 2008, **130**, 5854–5855.

10 L. M. Aguirre-Díaz, M. Iglesias, N. Snejko, E. Gutiérrez-Puebla and M. Á. Monge, *CrystEngComm*, 2013, **15**, 9562–9571.

11 S. Horike, M. Dinca, K. Tamaki and J. R. Long, *J. Am. Chem. Soc.*, 2008, **130**, 5854–5855.

12 (*a*) S. J. Geier, J. A. Mason, E. D. Bloch, W. L. Queen, M. R. Hudson, C. M. Brown and J. R. Long, *Chem. Sci.*, 2013, **4**, 2054–2061; (*b*) D. F. Sun, S. Q. Ma, Y. X. Ke, D. J. Collins and H. C. Zhou, *J. Am. Chem. Soc.*, 2006, **128**, 3896–3897; (*c*) W. Y. Gao, Y. Chen, Y. H. Niu, K. Williams, L. Cash, P. J. Perez, L. Wojtas, J. F. Cai, Y. S. Chen and S. Q. Ma, *Angew. Chem., Int. Ed.*, 2014, **53**, 2615–2619; (*d*) V. Colombo, S. Galli, H. J. Choi, G. D. Han, A. Maspero, G. Palmisano, N. Masciocchi and J. R. Long, *Chem. Sci.*, 2011, **2**, 1311–1319.

13 (*a*) L. J. McCormick, S. G. Duyker, A. W. Thornton, C. S. Hawes, M. R. Hill, V. K. Peterson, S. R. Batten and D. R. Turner, *Chem. Mater.*, 2014, **26**, 4640–4646; (*b*) Y. S. Bae, C. Y. Lee, K. C. Kim, O. K. Farha, P. Nickias, J. T. Hupp, S. T. Nguyen and R. Q. Snurr, *Angew. Chem., Int. Ed.*, 2012, **124**, 1857–1860; (*c*) B. L. Chen, S. C. Xiang and G. D. Qian, *Acc. Chem. Res.*, 2010, **43**, 1115–1124.

14 (*a*) K. Sumida, M. R. Hill, S. Horike, A. Dailly and J. R. Long, *J. Am. Chem. Soc.*, 2009, **131**, 15120–15121; (*b*) D. Saha, T. Maity, S. Das and S. Koner, *Dalton Trans.*, 2013, 13912–13922; (*c*) X. Q. Kong, E. Scott, W. Ding, J. A. Mason, J. R. Long and J. A. Reimer, *J. Am. Chem. Soc.*, 2012, **134**, 14341–14344.

15 D. Banerjee and J. B. Parise, *Cryst. Growth Des.*, 2011, **11**, 4704–4720.

16 (*a*) L. E. Kreno, K. Leong, O. K. Farha, M. Allendorf, R. P. van Duyne and J. T. Hupp, *Chem. Rev.*, 2012, **112**, 1105–1125; (*b*) Y. J. Cui, Y. F. Yue, G. D. Qian and B. L. Chen, *Chem. Rev.*, 2012, **112**, 1126–1162; (*c*) Z. C. Hu, B. J. Deibert and J. Li, *Chem. Soc. Rev.*, 2014, **43**, 5815–5840.

17 (*a*) B. Chen, Y. Yang, F. Zapata, G. Lin, G. Qian and E. B. Lobkovsky, *Adv. Mater.*, 2007, **19**, 1693–1696; (*b*) B. Chen, L. Wang, F. Zapata, G. Qian and E. B. Lobkovsky, *J. Am. Chem. Soc.*, 2008, **130**, 6718–6719; (*c*) B. Chen, L. Wang, Y. Xiao, F. R. Fronczek, M. Xue, Y. Cui and G. A. Qian, *Angew. Chem., Int. Ed.*, 2009, **48**, 500–503; (*d*) J. H. Wang, M. Li and D. Li, *Chem. Sci.*, 2013, **4**, 1793–1801; (*e*) J. Xiao, Y. Wu, M. Li, B. Y. Liu, X. C. Huang and D. Li, *Chem.–Eur. J.*, 2013, **19**, 1891–1895.

18 A. L. Spek, *J. Appl. Crystallogr.*, 2003, **36**, 7–13.

19 C. L. Chen, A. M. Goforth, M. D. Smith, C. Y. Su and H. C. Z. Loye, *Angew. Chem., Int. Ed.*, 2005, **44**, 6673–6677.

20 R. J. H. Gregory, *Chem. Rev.*, 1999, **99**, 3649–3682.

21 (*a*) M. Gustafsson, A. Bartoszewicz, B. Martín-Matute, J. L. Sun, J. Grins, T. Zhao, Z. Y. Li, G. S. Zhu and X. D. Zou, *Chem. Mater.*, 2010, **22**, 3316–3322; (*b*) F. Gándara, B. Gómez-Lor, M. Iglesias, N. Snejko,

E. Gutiérrez-Puebla and A. Monge, *Chem. Commun.*, 2009, 2393–2395; (*c*) Y. Zhu, Y. M. Wang, S. Y. Zhao, P. Liu, C. Wei, Y. L. Wu, C. K. Xia and J. M. Xie, *Inorg. Chem.*, 2014, **53**, 7692–7699; (*d*) H. F. Yao, Y. Yang, H. Liu, F. G. Xi and E. Q. Gao, *J. Mol. Catal. A: Chem.*, 2014, **394**, 57–65.

22 (*a*) G. Rajagopal, S. Selvaraj and K. Dhahagani, *Tetrahedron: Asymmetry*, 2010, **21**, 2265–2270; (*b*) S. A. Pourmousavi and H. Salahshornia, *Bull. Korean Chem. Soc.*, 2011, **32**, 1575–1578.

23 (*a*) I. Omae, *Coord. Chem. Rev.*, 2012, **256**, 1384–1405; (*b*) M. Cokoja, C. Bruckmeier, B. Rieger, W. A. Herrmann and F. E. Kühn, *Angew. Chem., Int. Ed.*, 2011, **50**, 8510–8537.

24 (*a*) T. Lescouet, C. Chizallet and D. Farrusseng, *ChemCatChem*, 2012, **4**, 1725–1728; (*b*) Y. W. Ren, Y. C. Shi, J. X. Chen, S. R. Yang, C. R. Qi and H. F. Jiang, *RSC Adv.*, 2013, **3**, 2167–2170; (*c*) W. Y. Gao, Y. Chen, Y. Niu, K. Williams, L. Cash, P. J. Perez, L. Wojtas, J. F. Cai, Y. S. Chen and S. Q. Ma, *Angew. Chem., Int. Ed.*, 2014, **53**, 2615–2619.

25 (*a*) V. Guillerm, Ł. J. Weseliński, Y. Belmabkhout, A. J. Cairns, V. D'Elia, Ł. Wojtas, K. Adil and M. Eddaoudi, *Nat. Chem.*, 2014, **6**, 673–680; (*b*) X. Q. Huang, Y. F. Chen, Z. G. Lin, X. Q. Ren, Y. N. Song, Z. Z. Xu, X. M. Dong, X. G. Li, C. W. Hu and B. Wang, *Chem. Commun.*, 2014, **50**, 2624–2627; (*c*) H. Y. Cho, D. A. Yang, J. Kim, S. Y. Jeong and W. S. Ahn, *Catal. Today*, 2012, **185**, 35–40.

26 (*a*) M. D. Allendorf, C. A. Bauer, R. K. Bhaktaa and R. J. T. Houka, *Chem. Soc. Rev.*, 2009, **38**, 1330–1352; (*b*) V. W. W. Yam, *Acc. Chem. Res.*, 2002, **35**, 555–563.

27 S. E. Denmark, J. P. Edwards and S. R. Wilson, *J. Am. Chem. Soc.*, 1991, **113**, 723–725.

